

Net quark number probability distribution near the chiral crossover transition

Kenji Morita,^{1,2,*} Bengt Friman,³ Krzysztof Redlich,^{4,2} and Vladimir Skokov⁵

¹*Yukawa Institute for Theoretical Physics, Kyoto University, Kyoto 606-8502, Japan*

²*Extreme Matter Institute EMMI, GSI, Planckstr. 1, D-64291 Darmstadt, Germany*

³*GSI, Helmholtzzentrum für Schwerionenforschung, Planckstr. 1, D-64291 Darmstadt, Germany*

⁴*Institute of Theoretical Physics, University of Wrocław, PL-50204 Wrocław, Poland*

⁵*Physics Department, Brookhaven National Laboratory, Upton, NY 11973, USA*

(Dated: February 24, 2022)

We investigate properties of the probability distribution of the net quark number near the chiral crossover transition in the quark-meson model. The calculations are performed within the functional renormalization group approach, as well as in the mean-field approximation. We find, that there is a substantial influence of the underlying chiral phase transition on the properties of the probability distribution. In particular, for a physical pion mass, the distribution which includes the effect of mesonic fluctuations, differs considerably from both, the mean-field and Skellam distributions. The latter is considered as a reference for a non-critical behavior. A characteristic feature of the net quark number probability distribution is that, in the vicinity of the chiral crossover transition in the $O(4)$ universality class, it is narrower than the corresponding mean-field and Skellam function. We study the volume dependence of the probability distribution, as well as the resulting cumulants, and discuss their approximate scaling properties.

PACS numbers: 25.75.Nq, 25.75.Gz, 24.60.-k, 12.39.Fe

I. INTRODUCTION

The structure of the QCD phase diagram is one of the fundamental problems addressed in both theoretical and experimental studies [1, 2]. At finite chemical potential, the existence of a critical point (CP) has been conjectured, based on effective chiral models [3] and preliminary lattice QCD results [4]. The fluctuations of conserved charges, have been proposed as a signature for the conjectured CP [5–10]. However, in this paper we focus on the QCD phase transition at small net baryon densities.

It was conjectured by Pisarski and Wilczek [11] that for massless light quarks, the QCD phase transition is of the second order, belonging to the $O(4)$ universality class. Current lattice QCD simulations at physical quark masses show, that at vanishing baryon density the transition from a hadron gas to quark matter is of the crossover type [12]. This implies that the corresponding singularity in the thermodynamic observables is shifted to complex values of the baryon chemical potential [13] and the experimental signatures of the phase transition could be washed out.

The conjecture of Pisarski and Wilczek is supported by recent lattice QCD studies [14, 15], which show that for physical values of the light quark masses, the magnetic equation of state of QCD is consistent with the $O(4)$ scaling. This result has opened new opportunities to verify the QCD phase boundary experimentally by measur-

ing fluctuations of conserved charges [5, 16–20]. Indeed, based on the residual $O(4)$ criticality and the proximity of the chiral crossover transition to the freeze-out line in heavy ion collisions, the characteristic modifications of the fluctuations of conserved charges have been proposed as a signature for the QCD phase boundary at small net baryon densities [5, 8, 16, 21–23]. It has been shown, that at the chiral crossover transition, the higher order cumulants of the net baryon number and electric charge can be negative, owing to the $O(4)$ scaling [22, 23].

Such cumulants have recently been explored in heavy ion collisions by STAR Collaboration [24, 25]. The data show deviations from the Skellam distribution, which are qualitatively consistent with theoretical expectations based on the $O(4)$ chiral critical dynamics. We note, however, that the role of uncertainties associated with the event-by-event measurements of fluctuations remain to be clarified [26–29].

Cumulants of net charges have also been studied in first principle lattice QCD calculations [19, 20, 30–32], as well as in effective chiral models [21–23, 33–40]. Their properties are consistent with general expectations based on the $O(4)$ scaling free energy.

Fluctuations of conserved charges are directly linked to the corresponding probability distribution. Thus, the critical properties of cumulants of conserved charges must also be reflected in the probability distribution.

Recently, the effects of the chiral phase transition on the net baryon number probability distribution was examined within the framework of mean-field theory and the scaling theory of phase transitions [41]. It was found, that the critical behavior of the cumulants is a consequence of the change of the corresponding probability distribution.

In the present work, we extend our previous studies

*Electronic address: kmorita@yukawa.kyoto-u.ac.jp; Present address: Frankfurt Institute for Advanced Studies, Ruth-Moufang-Str. 1, D-60438 Frankfurt am Main, Germany

to a more realistic model. We consider the two-flavor quark-meson model which is a low energy effective theory for the chiral properties of QCD. The critical fluctuations, are treated consistently by means of the functional renormalization group (FRG) [42–44].

In the quark-meson model the coupling of quarks to the Polyakov loop, which is important for implementation of the statistical confinement properties, is neglected. However, within the FRG approach, the $O(4)$ scaling behavior and thermodynamics near the CP are well described by this model [45–48].

We show that there is a substantial influence of the underlying chiral phase transition on the properties of the probability distribution. In particular, we find that for a physical pion mass, the distribution which includes the effect of mesonic fluctuations, differs considerably from both, the mean-field and Skellam distributions. The latter is considered as a reference for a non-critical behavior. A characteristic feature of the net quark number probability distribution is that in the vicinity of a chiral crossover transition of the $O(4)$ universality class, it is narrower than the corresponding mean-field and Skellam distributions.

This paper is organized as follows: in the next section, we introduce the quark-meson model and its thermodynamic properties. In Sec. III, we present results on the probability distribution and different cumulants of the net quark number. Section IV is devoted to the concluding remarks.

II. THE THERMODYNAMIC POTENTIAL IN THE QUARK-MESON MODEL

We employ the quark-meson model to explore the influence of the chiral phase transition on the probability

distribution of the net quark-number.

The quark-meson model is an effective realization of low energy QCD in which the $O(4)$ chiral meson multiplet $\phi = (\sigma, \vec{\pi})$ is coupled to quark fields. The Lagrangian density is given by

$$\mathcal{L} = \bar{q}[i\gamma_\mu\partial^\mu - g(\sigma + i\gamma_5\vec{\tau} \cdot \vec{\pi})]q + \frac{1}{2}(\partial_\mu\sigma)^2 + \frac{1}{2}(\partial_\mu\vec{\pi})^2 - U(\sigma, \vec{\pi}), \quad (1)$$

where $U(\sigma)$ denotes the meson potential,

$$U(\sigma, \vec{\pi}) = \frac{1}{2}m^2\phi^2 + \frac{\lambda}{4}\phi^4 - h\sigma. \quad (2)$$

For $m^2 < 0$ and $h = 0$, the $O(4)$ symmetry of the potential is spontaneously broken to $O(3)$, resulting in a non-vanishing value of the vacuum scalar condensate $\langle\sigma\rangle$ and a non-zero quark mass. The last term, $h = f_\pi m_\pi^2$, breaks the chiral symmetry explicitly and yields the nonzero pion mass.

We obtain the thermodynamics of the quark-meson model by computing the thermodynamic potential within the FRG approach, as discussed in Ref. [45]. Following [42], we consider a scale dependent effective action in the local potential approximation. Thereby, we neglect the wave function renormalization and the flow of the Yukawa coupling. Using the so-called optimized cutoff functions, one obtains the evolution equation for the scale dependent thermodynamic potential density [45] with the reduced field variable $\rho = (\sigma^2 + \vec{\pi}^2)/2$,

$$\partial_k\Omega_k(\rho) = \frac{k^4}{12\pi^2} \left[\frac{3}{E_\pi} \{1 + 2n_B(E_\pi)\} + \frac{1}{E_\sigma} \{1 + 2n_B(E_\sigma)\} - \frac{2\nu_q}{E_q} \{1 - n_F(E_q^+) - n_F(E_q^-)\} \right], \quad (3)$$

where n_B and n_F are the Bose and the Fermi distribution functions, respectively and $\nu_q = 2N_c N_f = 12$ is the quark degeneracy. The single particle energies of pion, sigma meson and quark/antiquark are given by

$$E_\pi = \sqrt{k^2 + \bar{\Omega}'_k}, \quad E_\sigma = \sqrt{k^2 + \bar{\Omega}'_k + 2\rho\bar{\Omega}''_k}, \quad E_q^\pm = \sqrt{k^2 + 2g^2\rho} \pm \mu, \quad (4)$$

where $\bar{\Omega}'_k$ and $\bar{\Omega}''_k$ denote the first and the second derivatives of $\bar{\Omega}_k = \Omega_k + h\sqrt{2\rho_k}$, with respect to ρ . The flow equation (3) is solved by using the Taylor expansion method. Expanding the potential up to the third order in ρ around the potential minimum ρ_k ,

$$\Omega_k(\rho) = \sum_{n=0}^3 \frac{a_n(k)}{n!} (\rho - \rho_k)^n, \quad (5)$$

and using Eq. (3), one finds the flow equations for the

coefficients $a_n(k)$ and ρ_k ,

$$\begin{aligned} d_k a_{0,k} &= \frac{c}{\sqrt{2\rho_k}} d_k \rho_k + \partial_k \Omega_k, \\ d_k \rho_k &= -\frac{1}{(c/(2\rho_k)^{3/2} + a_{2,k})} \partial_k \Omega'_k, \\ d_k a_{2,k} &= a_{3,k} d_k \rho_k + \partial_k \Omega''_k, \\ d_k a_{3,k} &= \partial_k \Omega'''_k, \end{aligned} \quad (6)$$

where $d_k = d/dk$. The flow equations are solved numerically starting at the ultraviolet cutoff scale $\Lambda = 1.0$ GeV [45]. We eliminate a_1 by means of the scale independent relation $h = a_1(k)\sqrt{2\rho_k}$.

There are four initial conditions for the flow equations, which are fixed at the scale $k = \Lambda$. Within this scheme, the initial value of a_0 is just a constant shift of thermodynamic potential Ω . We note, however, that such a cutoff at a finite momentum leads to an unphysical behavior of thermodynamic quantities at high temperatures. This problem can be amended by accounting for the μ - and T -dependent contribution of the momenta beyond the cutoff scale [37, 49]. Following Ref. [49], we include the high-momentum contribution approximately by using the flow equation for non-interacting massless quarks and gluons,

$$\partial_k \Omega_k^\Lambda(T, \mu) = \frac{k^3}{12\pi^2} \{2(N_c^2 - 1)[1 + 2n_B(k)] - \nu_q[1 - n_F(k^+) - n_F(k^-)]\}. \quad (7)$$

By integrating the flow equation (7) from $k = \infty$ to $k = \Lambda$, we obtain $\Omega^\Lambda(T, \mu)$ which is then used as initial condition $a_0(\Lambda)$ for the solution of the flow equations (6).

We set $a_3(\Lambda) = 0$ and fix $\rho_{k=\Lambda}$ and $a_2(\Lambda)$ by requiring that in vacuum the pion $m_\pi = 135$ MeV and the sigma $m_\sigma = 640$ MeV masses are reproduced. The strength of the Yukawa coupling, $g = 3.2$, is fixed by the constituent quark mass, $M_q(T = \mu = 0) = g\sigma_{k=0}(T = \mu = 0) = 300$ MeV with $\sigma_{k=0}(T = \mu = 0) = f_\pi = 93$ MeV. The full thermodynamic potential density of the quark-meson model $\Omega(T, \mu)$, which includes thermal and quantum fluctuations of the meson and quark fields, is then obtained from $\Omega(T, \mu) = \lim_{k \rightarrow 0} \Omega_k$, where Ω_k is the solution of the flow equation (3),(6).

By ignoring the mesonic contribution in the flow equation (3), we obtain the effective potential corresponding to the mean-field approximation, with a finite cutoff Λ . The fermionic vacuum fluctuations, which are included in the mean-field (MF) potential, are necessary to reproduce the second order phase transition at vanishing μ in the chiral limit [21, 46]. The vacuum contribution must be renormalized to remove the artificial cutoff dependence [21]. Then, in the mean-field approximation, the thermodynamic potential is given by,

$$\Omega_{\text{MF}}(\langle\sigma\rangle; T, \mu) = U(\langle\sigma\rangle, \vec{\pi} = 0) - \frac{\nu_q}{16\pi^2} M_q^4 \ln\left(\frac{M_q}{M}\right) - \nu_q T \int \frac{d^3p}{(2\pi)^3} \left[\ln(1 + e^{-(E_q - \mu)/T}) + \ln(1 + e^{-(E_q + \mu)/T}) \right], \quad (8)$$

where M is an arbitrary renormalization scale parameter, $M_q = g\langle\sigma\rangle$ and the expectation value $\langle\sigma\rangle$ is determined by the solution of the gap equation $\partial\Omega_{\text{MF}}/\partial\langle\sigma\rangle = 0$.

III. PROBABILITY DISTRIBUTION OF THE NET QUARK NUMBER

The thermodynamical potentials for the quark-meson model, derived in the previous section, can be used to assess the influence of the underlying chiral phase transition on observables. In the following, we focus on the probability distribution of the net quark number, $P(N)$ and the corresponding cumulants $c_n(T, \mu)$.

A. General properties of $P(N)$

We consider a thermodynamic system described by the grand canonical ensemble at temperature T in a subvolume V . We introduce a chemical potential μ which is used to tune the corresponding average net charge. For the net quark number $N = N_q - N_{\bar{q}}$, the probability distribution $P(N)$ to find the net charge N in volume V is given by

$$P(N; T, \mu, V) = \frac{Z(T, N, V)}{\mathcal{Z}(T, \mu, V)} e^{\mu N/T}, \quad (9)$$

where $Z(T, N, V)$ is the canonical and $\mathcal{Z}(T, \mu, V)$ the grand-canonical partition function. The normalization of the probability distribution, $\sum_{N=-\infty}^{\infty} P(N) = 1$, follows from the fugacity expansion of the grand canonical partition function

$$\mathcal{Z}(T, \lambda, V) = \sum_N \lambda^N Z(T, N, V), \quad (10)$$

where $\lambda = e^{\mu/T}$. Consequently, all essential information on $P(N)$ is contained in the canonical partition function. Since the fugacity expansion is the Laurent series in the complex λ plane, with coefficients given by the canonical partition function, the latter can be obtained by performing the contour integral,

$$Z(T, N, V) = \frac{1}{2\pi i} \oint_C d\lambda \frac{\mathcal{Z}(T, \lambda, V)}{\lambda^{N+1}}. \quad (11)$$

Thus, to compute the canonical partition function, one needs to know the analytic structure of $\mathcal{Z}(T, \lambda, V)$ in the complex λ plane and to choose an appropriate integration contour.¹ In chiral effective models, the structure of the singularities associated with the chiral phase transition has been discussed in Refs. [13, 50]. In the broken phase, $T < T_c(\mu)$, there are no singularities on the unit circle $\lambda = e^{i\theta}$ in the range $0 \leq \theta < 2\pi$. Consequently, the canonical partition function is obtained from [51, 52],

$$Z(T, N, V) = \frac{1}{2\pi} \int_0^{2\pi} d\theta e^{-i\theta N} \mathcal{Z}(T, \theta, V), \quad (12)$$

¹ In a finite system, the grand partition function \mathcal{Z} has Yang-Lee zeroes at complex values of λ . In the thermodynamic limit, the zeroes join into cuts.

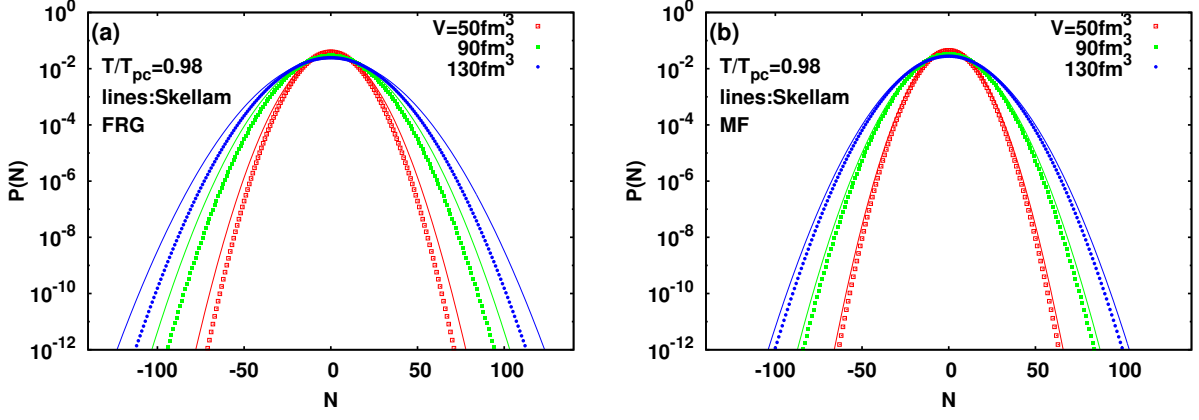


FIG. 1: (Color online) Probability distributions of the net quark number just below the pseudocritical temperature T_{pc} (a) in the FRG approach and (b) in the mean-field (MF) approximation, compared with the corresponding Skellam distributions. The dots are the model results for different volumes while the lines show the Skellam distribution.

where $\theta = \mu_I/T$ and μ_I is the imaginary chemical potential.

The above equation links the grand canonical partition function in a finite volume V , at imaginary chemical potential, to the thermodynamics at fixed net charge N . At imaginary μ_I , the QCD partition function exhibits Roberge-Weiss periodicity, $\mathcal{Z}(T, \theta + 2\pi/3, V) = \mathcal{Z}(T, \theta, V)$ [53]. The Polyakov loop extended effective chiral models reproduce the Roberge-Weiss periodicity [54–56]. In the quark-meson model employed here, the period of the partition function in imaginary chemical potential θ is 2π .

In the present work, we follow Ref. [41] and compute the canonical partition function and the corresponding probability distribution using Eq. (12). The thermodynamic potential density $\Omega = -(T/V) \log \mathcal{Z}$ is obtained in the quark-meson model within the FRG approach as well as in the mean-field approximation.

Because of the oscillatory nature of the integrand, a numerical integration of Eq. (12) becomes unreliable for large $|N|$. The numerical quadrature employed here yields accurate results up to values of $|N|$ corresponding to $P(N; \mu = 0) \sim 10^{-12}$, independent of the volume, temperature and other parameters. As we show, the achieved precision is sufficient for studying the influence of chiral criticality on the properties of the net quark number probability distribution.

B. Net quark number probability distribution near the chiral phase transition

At vanishing and moderate values of μ , the quark-meson model in the chiral limit exhibits the second order phase transition, belonging to the $O(4)$ universality class [45]. For a physical pion mass, the chiral symmetry is explicitly broken and the transition is of the crossover type. Nevertheless, remnants of $O(4)$ criticality remain in various observables [5]. Thus, also the probability dis-

tribution of the net quark number is expected to exhibit characteristic features reflecting the critical behavior of the underlying $O(4)$ transition. We note, that long range critical correlations can be unfolded only in a sufficiently large sub-volume V , and close to the pseudocritical temperature, T_{pc} .

To unravel the influence of chiral transition on the probability distribution $P(N)$, one needs to establish a reference distribution, which does not include the effect of critical fluctuations. At low temperatures, $T \ll T_{pc}$, the thermodynamic potential is expected to be well described as a quasi-ideal quark gas with a dynamically generated temperature-dependent mass. Consequently, at fixed T and V , the natural reference for $P(N)$ is the probability distribution of an ideal gas of particles and antiparticles, i.e. the Skellam distribution [16]. The Skellam distribution is then determined entirely by the mean number of quarks $b = \langle N_q \rangle$ and antiquarks $\bar{b} = \langle N_{\bar{q}} \rangle$,

$$P(N) = \left(\frac{b}{\bar{b}}\right)^{N/2} I_N(2\sqrt{b\bar{b}}) e^{-(b+\bar{b})}, \quad (13)$$

where $I_N(x)$ is the modified Bessel function of the first kind. The mean number of quarks b is calculated as for an ideal gas of constituent quarks with a dynamically generated mass

$$b = \frac{\nu_q V}{2\pi^2} \int_0^\infty dk k^2 n_F(E_k; T, \mu), \quad (14)$$

where n_F is the Fermi distribution function and $E_k = \sqrt{k^2 + M_q^2}$ is the energy of a particle with momentum k . The \bar{b} is obtained from (14) by replacing $\mu \rightarrow -\mu$.

In the MF approximation $M_q = g\langle\sigma\rangle$, while in the FRG approach, we use the scale dependent mass $M_{q,k} = g\sigma_k$, which for $k \leq \Lambda$ is obtained from the flow equation (3). For $\Lambda < k < \infty$ the quarks are assumed to be massless and non-interacting, as discussed above.

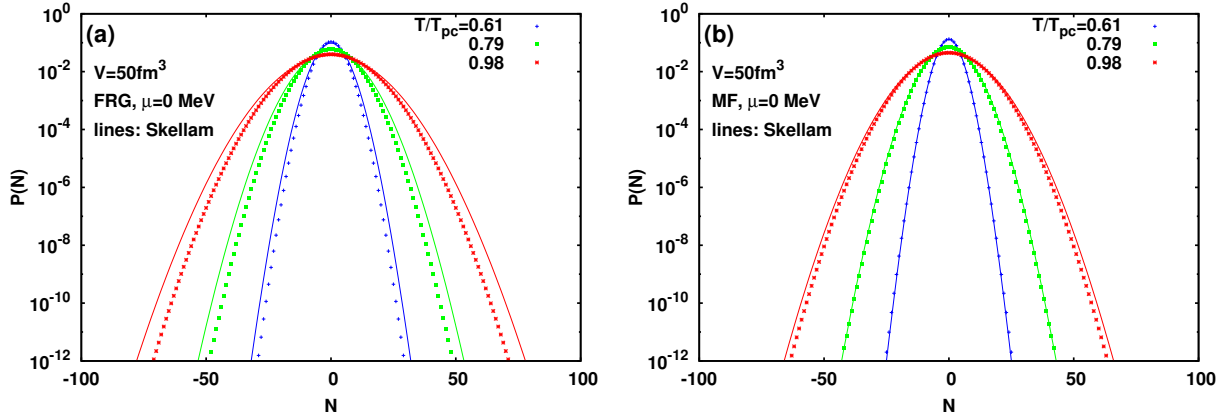


FIG. 2: (Color online) Probability distribution for different temperatures (a) in the FRG approach and (b) in the mean-field (MF) approximation. The dots are the model results while the lines show the corresponding Skellam distribution (see text).

Figure 1 shows the probability distributions of the net quark number obtained in the quark-meson model, within the FRG and in the MF approximation at vanishing chemical potential and near the pseudocritical temperature T_{pc} . The T_{pc} corresponds to the peak position of the chiral susceptibility, which in the FRG and MF calculations are located at 214 MeV and 190 MeV, respectively.

The probability distributions in Fig. 1 are calculated for different volumes and at fixed temperature. There is a clear change of distributions with the volume as a consequence of a linear dependence of the variance on V . The probability distribution also changes rapidly as the temperature is lowered from the pseudocritical point. As shown in Fig. 2, at a given volume, the distributions are narrower at smaller temperatures. This is due to growing mass of quarks, which together with decreasing temperature, imply decreasing mean number of quarks and antiquarks, and consequently the width of the distribution.

The influence of the criticality on the net-quark number probability distribution, and the differences between the MF and the FRG dynamics, are particularly transparent when comparing the results with the non-critical Skellam function.

Figures 1 and 2 show, that near T_{pc} , both the MF and the FRG distributions are narrower than their Skellam counterparts. Such reduction of the width of the probability distribution compared to the Skellam distribution was already seen in results obtained previously in the Landau theory of phase transitions when critical fluctuation is included to give negative higher order cumulants [41]. The deviations from Skellam distribution are stronger when mesonic fluctuations are included, i.e. in the FRG approach. Except for the highest temperature, $P(N)$ in the MF approximation coincides with the Skellam distribution, while in the FRG calculations, the two distributions differ at all temperatures. The increasing difference between the FRG and Skellam distributions,

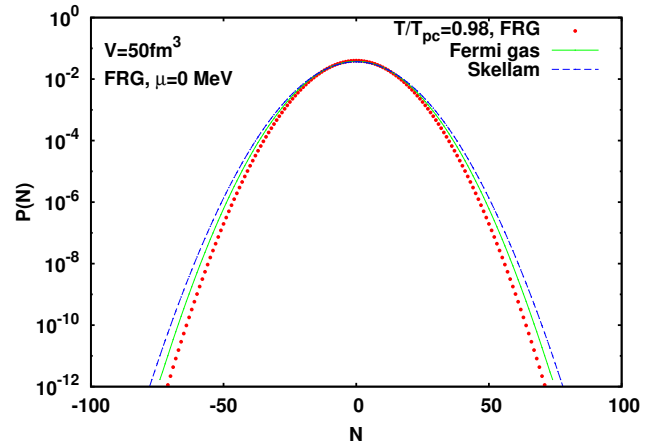


FIG. 3: (Color online) The probability distribution obtained within the FRG approach (red, circles), the Skellam distribution (blue, dashed), and that of a free Fermi gas (green, solid). All distributions correspond to the same average quark and antiquark numbers, b and \bar{b} , given by (14).

as the temperature approaches T_{pc} , reflects the growing influence of mesonic fluctuations leading to the $O(4)$ criticality.

C. Quantum statistics effects

The Skellam distribution (13), describes the fluctuations in a gas of non-interacting classical particles with a conserved charge. *i.e.*, particles and antiparticles obeying the Poisson distribution.

In general, effects of quantum statistics should be included if the mass of the particle is smaller than the temperature. The quantum statistics effects were also shown to modify significantly the probability distribution of the electric charge and the resulting cumulants [17, 57].

In the FRG approach to the quark-meson model, and

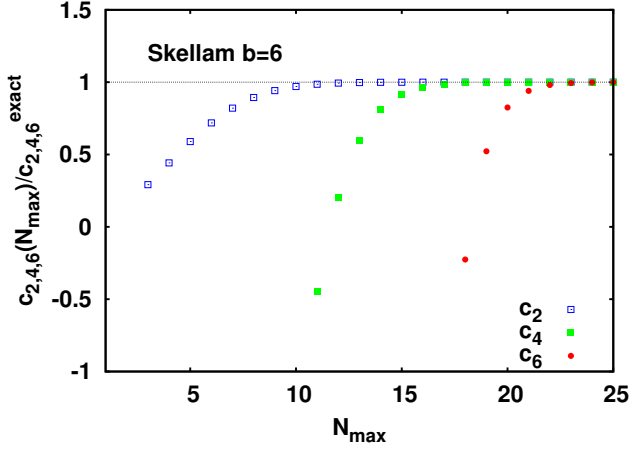


FIG. 4: (Color online) The ratios of the cumulants c_n ($n = 2, 4, 6$) of the net charge obtained from the Skellam distribution with the mean multiplicities $b = \bar{b} = 6.0$ using Eqs. (17)-(20) for a given value of N_{\max} to their corresponding exact values.

at $T/T_{pc} = 0.98$ one finds, that $M_q/T \simeq 0.6$. Thus, the Boltzmann approximation is clearly not justified near T_{pc} .

In order to disentangle the effects of mesonic fluctuations and quantum statistics, we also consider the probability distribution $P(N)$, obtained from Eq. (12), for a free gas of quarks and anti-quarks with the thermodynamic potential density

$$\Omega_{\text{Fermi}}(T, \theta) = -\frac{\nu_q T}{2\pi^2} \int_0^\infty dk k^2 [\ln(1 + e^{-E_k/T + i\theta}) + \ln(1 + e^{-E_k/T - i\theta})], \quad (15)$$

and the quark energy E_k from Eq. (14).

The effect of Fermi statistics is illustrated in Fig. 3 with the dynamical quark mass obtained in the FRG approach. The probability distribution of the free Fermi gas is seen to be narrower than the corresponding Skellam function, but still broader than the $P(N)$ of the quark-meson model in the FRG approach. We identify the residual effect, i.e. the difference between the Fermi gas and the FRG distributions, as being due to the mesonic fluctuations implying the $O(4)$ criticality near the chiral crossover transition.

On the other hand, in the MF approach at $T/T_{pc} = 0.98$, the net-quark probability distribution was found to be slightly broader than the corresponding distribution obtained for a free Fermi gas. Therefore, in the MF approach, the apparently narrower distribution than the Skellam, is due to the quantum statistics effects. Thus, there is a clear difference in the properties of the net-quark distributions obtained under MF and the FRG approach. The mesonic fluctuations result in a shrinking of the distribution, whereas the MF critical dynamics results in a broadening of the distribution, relatively to the

non-singular Fermi gas reference, as shown in [41].

D. Cumulants of the net quark number

Fluctuations of the net-quark number are quantified by the corresponding cumulants $c_n(T, \mu)$, which in turn reflect critical fluctuations. Consequently, cumulants can be used to probe the phase diagram of QCD [5, 8–10, 16, 21–23].

In statistical physics, the cumulants are related to the corresponding susceptibilities,

$$c_n(T, \mu) \equiv \frac{\partial^n [p(T, \mu)/T^4]}{\partial (\mu/T)^n}. \quad (16)$$

Thus, given the thermodynamic pressure $p(T, \mu, V) = (T/V) \ln \mathcal{Z}$ in the grand-canonical ensemble, the cumulants $c_n(T, \mu)$ can be obtained by taking derivatives of the thermodynamic pressure with respect to the chemical potential.

The cumulants in Eq. (16) can be also obtained from the probability distribution $P(N)$, through the central moments, $\langle (\delta N)^k \rangle = \langle (N - \langle N \rangle)^k \rangle$, where

$$\langle N^k \rangle = \sum_{N=-N_{\max}}^{N_{\max}} N^k P(N), \quad (17)$$

and c_n are given then as polynomials in $\langle (\delta N)^k \rangle$. At vanishing chemical potential, the first three non-vanishing cumulants read,

$$c_2 = \frac{\langle (\delta N)^2 \rangle}{VT^3}, \quad (18)$$

$$c_4 = \frac{\langle (\delta N)^4 \rangle - 3\langle (\delta N)^2 \rangle^2}{VT^3}, \quad (19)$$

$$c_6 = [\langle (\delta N)^6 \rangle - 15\langle (\delta N)^4 \rangle \langle (\delta N)^2 \rangle - 10\langle (\delta N)^3 \rangle^2 + 30\langle (\delta N)^2 \rangle^3] / (VT^3). \quad (20)$$

In principle, N_{\max} in Eq. (17) is infinite. In practice, however, N_{\max} is always finite. Thus, the cumulants obtained from Eqs. (17)-(20) are, in most cases, approximations to the exact results obtained from Eq. (16).

Figure 4 shows different ratios of cumulants for the Skellam distribution, calculated for fixed mean number of quarks and antiquarks, from Eqs. (17)-(20) for different N_{\max} . Clearly, to reproduce exact results $c_{2n} = (b + \bar{b})/VT^3$, one needs $P(N)$ for a sufficiently large $N = N_{\max}$. This value increases with the order of the cumulant, and also depends on the volume, temperature and the chemical potential.

Figure 5 shows different cumulants obtained in the quark-meson model within the FRG approach from Eq. (16) and their approximate values computed from Eqs. (17)-(20) as functions of temperature, for several values of N_{\max} . For comparison, the cumulants obtained from the corresponding Skellam distribution are

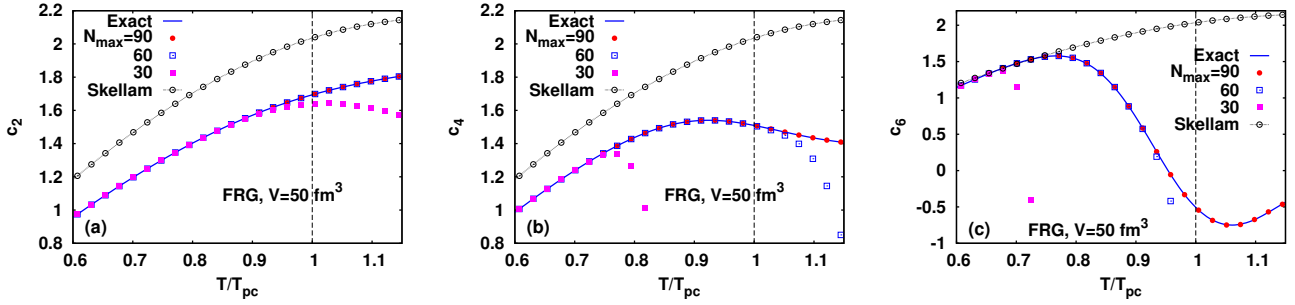


FIG. 5: (Color online) Cumulants c_n ($n = 2, 4, 6$) obtained in the quark-meson model within the FRG approach using Eq. (16) (full line) and Eqs. (17-20) (points) for several values of N_{max} . Results for the corresponding Skellam distribution are also indicated by the lines with open circles.

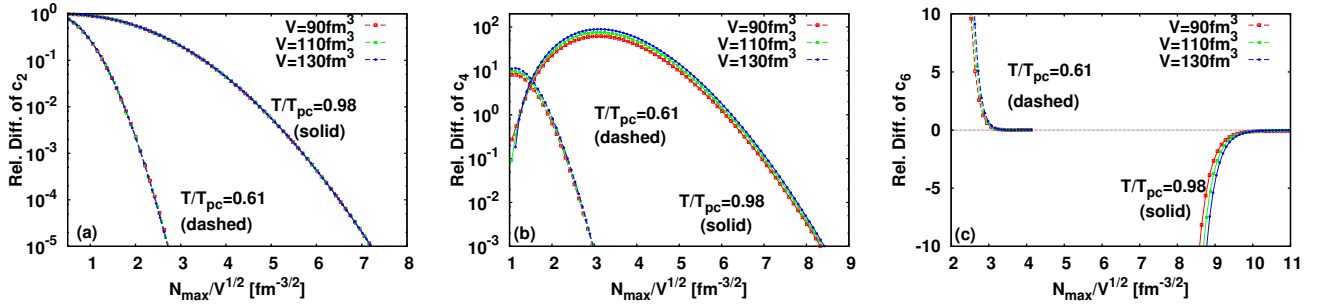


FIG. 6: (Color online) Relative difference between cumulants c_n ($n = 2, 4, 6$) calculated in the quark-meson model within the FRG approach using Eq. (16) and Eqs. (17-20) for two temperatures and for several values of the volume parameters V (see text).

also shown in this figure. One notes, that c_2 and c_4 of the Skellam and FRG distributions differ, while c_6 agrees for temperatures well below T_{pc} . This behavior can be linked to the μ -dependence of a dynamical quark mass, which at $T \ll T_{pc}$ saturates as the fourth order polynomial in μ , which is not included in the calculations of c_n from the Skellam function.

The convergence properties of the cumulants with N_{max} in the quark-meson model are similar to those found for the Skellam distribution. The value of N_{max} needed to obtain a good approximation, grows with the order of the cumulant. This reflects the fact, that cumulants of higher order are more sensitive to tail of the distribution. For the parameter set used in Fig. 5, all cumulants up to the sixth order are well reproduced with $N_{max} \simeq 90$. This also confirms consistency of the calculation of $P(N)$ within the quark-meson model.

At $\mu = 0$, the second and the fourth order cumulants are not influenced by the critical chiral dynamics, since they remain finite, even in the chiral limit. Thus, their properties are entirely determined by the regular part of the partition function. The temperature dependence of c_2 and c_4 , seen in Fig. 5, is essentially that of an ideal quark gas, with a modified dispersion relation by T - and μ -dependence of a dynamical quark mass.

In contrast, the temperature dependence of c_6 , and in

particular its negative values near T_{pc} , seen in Fig. 5, are universal. The characteristic shape of c_6 is generic for the $O(4)$ universality class, owing to the form of the scaling function [5]. The sixth order cumulant obtained from the non-critical Skellam distribution, exhibits a very different behavior.

It is interesting to note, that already for moderate values of N_{max} , the $O(4)$ shape of c_6 is qualitatively reproduced from the probability distribution. This result is of interest for the event-by-event analysis of heavy-ion collisions, where one expects to see the $O(4)$ criticality by reconstructing the higher order moments from the measured net-charge probability distribution [24].

The deviations of the approximate cumulants c_n^A , obtained from the probability distribution (17)-(20), from their exact values c_n^E , given by Eq. (16), depend on the volume of the system. The relative deviations of c_n^A from c_n^E at fixed T for different V , however, obey the approximate scaling relations. This is transparent from Fig. 6, showing the relative difference, $R = (c_n^E - c_n^A)/c_n^E$ for $n = 2, 4, 6$, as a function of N_{max}/\sqrt{V} . For $n = 2$ there is a clear scaling for all N_{max} . For higher order cumulants, the approximate scaling becomes better for larger values of N_{max}/\sqrt{V} .

Since the cumulants of the net quark number are linked to the corresponding probability distribution through

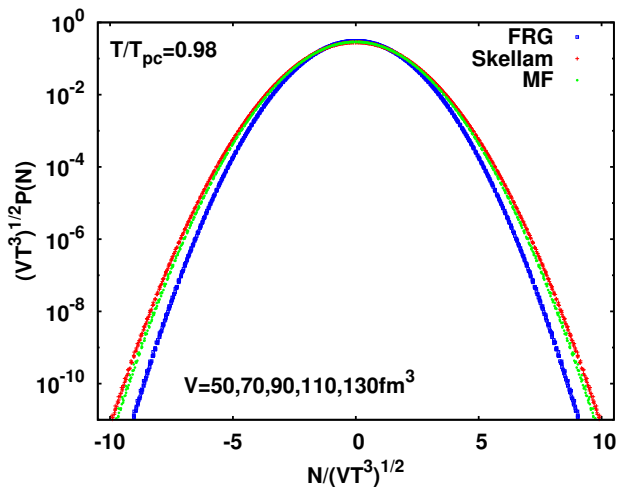


FIG. 7: (Color online) Volume scaling of the net quark number probability distribution at fixed T/T_{pc} in the quark-meson model within the MF, the FRG approach and for the corresponding Skellam distribution.

Eqs. (17)-(20), the approximate scaling of the cumulants, seen in Fig. 6, should be also reflected in the net quark number probability distributions. Indeed, Figure 7 shows, that for fixed T , the $\sqrt{VT^3}P(N)$ scales approximately with $N/\sqrt{VT^3}$. This approximate scaling is valid for $P(N)$, calculated in the quark-meson model within the FRG and MF approach, as well as, for the corresponding Skellam distributions. Figure 7 indicates, that the shape of the distribution reflects the underlying criticality in a system which is governed by the critical exponents. The probability distribution in the MF case is broader than in the FRG approach, owing to differences caused by the mesonic fluctuations. As they smoothen the transition, the resultant dynamical quark mass is heavier than the MF case at the same T/T_{pc} [37], leading to narrower distribution.

IV. CONCLUDING REMARKS

We have studied the properties of the probability distribution $P(N)$ of the net quark number in the presence of the critical chiral dynamics governed by the $O(4)$ universality class in the quark-meson model. The computations of $P(N)$ have been done within the Functional Renormalization Group (FRG) approach, which preserves the $O(4)$ scaling of relevant physical observables.

The main objectives of this paper was to study the influence of the underlying chiral phase transition on the net quark probability distribution, for a physical value of

the pion mass.

We have shown, by comparing the FRG and the mean-field (MF) results, that the shape of the distribution reflects the criticality in a system. The FRG distribution is narrower than the one obtained in the MF approximation. This is mainly due to differences in the values of dynamically generated quark mass. Effects of the expected $O(4)$ criticality appear in the tail of the distribution and imply characteristic shapes of the higher order cumulants.

Near the chiral crossover transition, the probability distribution of the net quark number was also shown to be narrower than the Skellam function, which corresponds to a classical quasiparticle gas and is used as a reference for the non-critical distribution. The narrowing of the probability distribution is mainly due to mesonic fluctuations. However, owing to dropping quark mass near the chiral transition also quantum statistics play a role, although a sub-leading one.

The observed shrinking of $P(N)$ relative to the Skellam distribution is also expected in the $O(2)$ universality class. This is because, the scaling functions in the $O(4)$ and $O(2)$ universality classes are very similar [14] and exhibit negative values of the specific heat critical exponents α . However, since α in $O(2)$ is larger than in $O(4)$ universality class, one expects quantitative differences in the properties of $P(N)$.

We have found an approximate scaling of the probability distribution and of the net charge cumulants with the volume of the system. This implies, that the observed properties of $P(N)$ near the chiral transition are volume independent, and are due to mesonic fluctuations implying $O(4)$ criticality near the chiral crossover transition.

These results are of importance in heavy ion collisions, where by measuring the net baryon number probability distribution and related moments, one expects to experimentally probe the QCD phase boundary. The phenomenological implications of our results will be presented elsewhere [58].

Acknowledgments

The authors acknowledge stimulating discussions with P. Braun-Munzinger, F. Karsch and Nu Xu. K.M. was supported by Yukawa International Program for Quark-Hadron Sciences at Kyoto University and by the Grant-in-Aid for Scientific Research from JSPS No.24540271. B.F. is supported in part by the Extreme Matter Institute EMMI. K.R. acknowledges partial support of the Polish Ministry of National Education (MEN). The research of V.S. is supported under Contract No. DE-AC02-98CH10886 with the U. S. Department of Energy.

[1] B. Friman, C. Höhne, J. Knoll, S. Leupold, J. Randrup, R. Rapp, and P. Senger, Lect. Note. Phys. **814**, 1 (2011).

[2] K. Fukushima and T. Hatsuda, Rep. Prog. Phys. **74**,

- 014001 (2011).
- [3] M. Asakawa and K. Yazaki, Nucl. Phys. **A504**, 668 (1989).
 - [4] Z. Fodor and S. D. Katz, JHEP **0203**, 014 (2002); C. Schmidt, C. R. Allton, S. Ejiri, S. J. Hands, O. Kaczmarek, F. Karsch and E. Laermann, Nucl. Phys. Proc. Suppl. **119**, 517 (2003); R. V. Gavai, Nucl. Phys. A **862**, 104 (2011).
 - [5] F. Karsch and K. Redlich, Phys. Lett. B **695**, 136 (2011).
 - [6] Y. Hatta and M. A. Stephanov, Phys. Rev. Lett. **91**, 102003 (2003).
 - [7] M. Stephanov, K. Rajagopal, and E. Shuryak, Phys. Rev. Lett. **81**, 4816 (1998).
 - [8] S. Ejiri, F. Karsch, and K. Redlich, Phys. Lett. B **633**, 275 (2006).
 - [9] M. A. Stephanov, Phys. Rev. Lett. **102**, 032301 (2009).
 - [10] M. A. Stephanov, Phys. Rev. Lett. **107**, 052301 (2011).
 - [11] R. D. Pisarski and F. Wilczek, Phys. Rev. D **29**, 338 (1984).
 - [12] Y. Aoki, G. Endrödi, Z. Fodor, S. D. Katz, and K. K. Szabó, Nature **443**, 675 (2006).
 - [13] V. Skokov, K. Morita, and B. Friman, Phys. Rev. D **83**, 071502(R) (2011); B. Friman, Acta. Phys. Pol. B (Proc Suppl.) **5**, 707 (2012).
 - [14] S. Ejiri, F. Karsch, E. Laermann, C. Miao, S. Mukherjee, P. Petreczky, C. Schmidt, W. Soeldner, and W. Unger, Phys. Rev. D **80**, 094505 (2009).
 - [15] A. Bazavov, T. Bhattacharya, M. Cheng, C. DeTar, H. T. Ding, S. Gottlieb, R. Gupta and P. Hegde *et al.*, Phys. Rev. D **85**, 054503 (2012).
 - [16] P. Braun-Munzinger, B. Friman, F. Karsch, K. Redlich, and V. Skokov, Phys. Rev. C **84**, 064911 (2011).
 - [17] P. Braun-Munzinger, B. Friman, F. Karsch, K. Redlich, and V. Skokov, Nucl. Phys. **A880**, 48 (2012).
 - [18] O. Kaczmarek, F. Karsch, E. Laermann, C. Miao, S. Mukherjee, P. Petreczky, C. Schmidt, W. Soeldner, and W. Unger, Phys. Rev. D **83**, 014504 (2011).
 - [19] A. Bazavov *et al.* (HotQCD Collaboration), Phys. Rev. D **86**, 034509 (2012).
 - [20] A. Bazavov, H. T. Ding, P. Hegde, O. Kaczmarek, F. Karsch, E. Laermann, S. Mukherjee and P. Petreczky *et al.*, Phys. Rev. Lett. **109**, 192302 (2012).
 - [21] V. Skokov, B. Friman, E. Nakano, K. Redlich, and B.-J. Schaefer, Phys. Rev. D **82**, 034029 (2010).
 - [22] B. Friman, F. Karsch, K. Redlich, and V. Skokov, Eur. Phys. J. C **71**, 1694 (2011).
 - [23] V. Skokov, B. Friman, and K. Redlich, Phys. Rev. C **83**, 054904 (2011).
 - [24] M. M. Aggarwal *et al.* (STAR Collaboration), Phys. Rev. Lett. **105**, 022302 (2010).
 - [25] X. Luo (STAR Collaboration), Nucl. Phys. **A904-905**, 911c (2013), L. Chen (STAR Collaboration), Nucl. Phys. **A904-905**, 471c (2013).
 - [26] M. Kitazawa and M. Asakawa, Phys. Rev. C **85**, 021901 (2012).
 - [27] M. Kitazawa and M. Asakawa, Phys. Rev. C **86** (2012) 024904 [Erratum-ibid. C **86** (2012) 069902].
 - [28] A. Bzdak, V. Koch and V. Skokov, Phys. Rev. C **87**, 014901 (2013).
 - [29] A. Bzdak and V. Koch, Phys. Rev. C **86**, 044904 (2012).
 - [30] C. R. Allton, M. Döring, S. Ejiri, S. J. Hands, O. Kaczmarek, F. Karsch, E. Laermann, and K. Redlich, Phys. Rev. D **71**, 054508 (2005).
 - [31] S. Borsanyi, Z. Fodor, S. D. Katz, S. Krieg, C. Ratti, and K. Szabo (Wuppertal-Budapest Collaboration), JHEP **1201**, 138 (2012).
 - [32] M. Cheng, P. Hegde, C. Jung, F. Karsch, O. Kaczmarek, E. Laermann, R. D. Mawhinney and C. Miao, P. Petreczky, C. Schmidt and W. Soeldner, Phys. Rev. D **79**, 074505 (2009).
 - [33] K. Fukushima, Phys. Lett. B **591**, 277 (2004).
 - [34] C. Sasaki, B. Friman, and K. Redlich, Phys. Rev. D **75**, 054026 (2007).
 - [35] C. Sasaki, B. Friman, and K. Redlich, Phys. Rev. D **75**, 074013 (2007).
 - [36] B. Stokic, B. Friman, and K. Redlich, Phys. Lett. B **673**, 192 (2009).
 - [37] V. Skokov, B. Stokic, B. Friman, and K. Redlich, Phys. Rev. C **82**, 015206 (2010).
 - [38] M. Asakawa, S. Ejiri, and M. Kitazawa, Phys. Rev. Lett. **103**, 262301 (2009).
 - [39] T. K. Herbst, J. M. Pawłowski, and B. J. Schaefer, Phys. Lett. B **696**, 58 (2011).
 - [40] B.-J. Schaefer and M. Wagner, Phys. Rev. D **85**, 034027 (2012); M. Wagner, A. Walther, and B.-J. Schaefer, Comp. Phys. Comm. **181**, 756 (2010).
 - [41] K. Morita, V. Skokov, B. Friman, and K. Redlich, arXiv:1211.4703 [hep-ph].
 - [42] C. Wetterich, Phys. Lett. B **301**, 90 (1993).
 - [43] J. Berges, N. Tetradis, and C. Wetterich, Phys. Rept **363**, 223 (2002).
 - [44] B. Delamotte, cond-mat/0702365.
 - [45] B. Stokić, B. Friman, and K. Redlich, Eur. Phys. J. C **67**, 425 (2010).
 - [46] E. Nakano, B. J. Schaefer, B. Stokic, B. Friman, and K. Redlich, Phys. Lett. B **682**, 401 (2010).
 - [47] B.-J. Schaefer and J. Wambach, Phys. Rev. D **75**, 085015 (2007).
 - [48] K. Kamikado, T. Kunihiro, K. Morita, and A. Ohnishi, Prog. Theor. Exp. Phys. **2013**, 053D01.
 - [49] J. Braun, H. -J. Pirner, K. Schwenzer, Phys. Rev. D **70**, 085016 (2004).
 - [50] M. A. Stephanov, Phys. Rev. D **73**, 094508 (2006).
 - [51] P. Braun-Munzinger, K. Redlich, and J. Stachel, in *Quark-Gluon Plasma 3*, edited by R. C. Hwa and X. N. Wang (World Scientific, 2004).
 - [52] R. Hagedorn and K. Redlich, Z. Phys. C **27**, 541 (1985).
 - [53] A. Roberge and N. Weiss, Nucl. Phys. **B275**, 734 (1986).
 - [54] Y. Sakai, K. Kashiwa, H. Kouno, and M. Yahiro, Phys. Rev. D **77**, 051901(R) (2008).
 - [55] K. Morita, V. Skokov, B. Friman, and K. Redlich, Phys. Rev. D **84**, 076009 (2011).
 - [56] K. Morita, V. Skokov, B. Friman, and K. Redlich, Phys. Rev. D **84**, 074020 (2011).
 - [57] V. Skokov, B. Friman and K. Redlich, Phys. Lett. B **708**, 179 (2012).
 - [58] K. Morita, talk given at The 4th Asian Triangle Heavy Ion Conference (ATHIC2012), November 16 2012, Pusan, Korea; K. Morita, B. Friman, K. Redlich, V. Skokov, in preparation.